Progress In Electromagnetics Research, PIER 102, 315–335, 2010

GENERALIZED 3D TRANSVERSE MAGNETIC MODE METHOD FOR ANALYSIS OF INTERACTION BETWEEN DRIFTING PLASMA WAVES IN 2DEG-STRUCTURED SEMICONDUCTORS AND ELECTROMAGNETIC SPACE HARMONIC WAVES

F. Mustafa and A. M. Hashim

Material Innovations and Nanoelectronics Research Group
Faculty of Electrical Engineering
Universiti Teknologi Malaysia
81310 Skudai, Johor, Malaysia

Abstract—Up to now, the terahertz (THz) band is still an unexplored region in the sense that no practical application exists. New operating principles by traveling wave concept should be, therefore, appreciated for the real applications. In this paper, the generalized three-dimensional (3D) transverse magnetic (TM) mode analysis to analyze the characteristics of two-dimensional electron gas (2DEG) drifting plasma at the III-V high-electron-mobility-transistor (HEMT) hetero-interface such as AlGaAs/GaAs hetero-interface and its interaction with propagating electromagnetic space harmonic wave is presented. It includes, (1) the determination of electromagnetic fields in semiconductor drifting plasma using the combination of well-known Maxwell's equations and carrier kinetic equation based on semiconductor fluid model and the derivation of the effective permittivity of drifting plasma in 2DEG on semi-insulating substrate, and (2) the analysis to describe the presence of interactions using a so-called interdigital-gated HEMT plasma wave devices. To describe the interaction, the admittance of the interdigital gate is evaluated. The numerical procedures to solve the integral equations which are used in determining the admittance is explained. A negative conductance is obtained when drifting carrier velocity is slightly exceed the fundamental wave velocity indicates the significant condition of the interaction. A brief analysis and discussion on the Dyakonov-Shur THz surface wave in 2DEG is also presented.

Corresponding author: A. M. Hashim (manaf@fke.utm.my).

1. INTRODUCTION

Being motivated by the tremendous success of traveling wave tubes (TWTs), the possibilities of obtaining an extremely large amplification of electromagnetic (EM) waves by utilizing a coupling between drifting carriers in semiconductor and EM waves propagating in slow-wave circuits were theoretically explored [1–4]. The idea is to replace the electron beam in a traveling wave tube with drifting carriers in a semiconductor. These drifting charge carriers in the semiconductor would interact with the slow electromagnetic waves resulting in a convective instability. Hence, there would be the possibility of constructing a new type electromagnetic wave amplifier by injecting a signal at one end of the semiconductor and taking out an augmented signal at the other end. All of this work was done in the 1960s and 1970s when semiconductor technology was still poor. These activities faded out without remarkable success mainly due to the strong collision dominant (CD) nature of semiconductor plasma as compared with electrons travelling in vacuum.

Due to significant progress in semiconductor material and device fabrication technologies, frequencies handled by conventional semiconductor devices have been remarkably enhanced, approaching terahertz (THz) frequencies where transit time limitation of those devices now imposes very severe limitations on the frequency and power capabilities of devices. In fact, the maximum cut-off frequency, f_T, obtained thus far in conventional devices still remains slightly above 500 GHz, even with the use of short gate lengths of a few nanometer [5]. In addition, it is also known that such transit time devices with reduced gate lengths show severe short-channel effects and large gate leakage currents [6, 7]. Thus, it is unlikely that such conventional devices will achieve operation in the THz region with acceptable performance.

Recently, the use of plasma waves for wave detection in THz region at low temperature supported by a non-drifting 2DEG with an AlGaAs/GaAs heterostructure under a metal gate which was proposed by Dyakonov and Shur [8] have been successfully demonstrated. There is also a stimulating work by Otsuji's group to apply this plasma wave concept into smart photonic network system [9]. Recently, we also demonstrated the THz wave detection at room temperature applying this non-drifting plasma theory [10].

In our previous publications on drifting plasma concept, we presented both the theoretical and experimental results of interdigital-gated plasma wave device fabricated on III-V bulk structure such as GaAs and InP [11]. It is noted here that the effective permittivity of those material systems are different from the III-V material systems

with 2DEG layer. The effects of quasi-lamellar electromagnetic field also need to be taken into account for bulk structure. We also presented some motivated results both theoretically and experimentally for the III-V material systems with 2DEG layer, specifically on AlGaAs/GaAs HEMT structure [12–15]. Since, the III-V HEMT structure is better than bulk structure for drifting plasma interaction and the comparison with the experimental results and reliable explanation and discussion have been established, the generalized transverse magnetic (TM) mode approach need to be presented and explained in detail for the readers to understand this drifting plasma concept compared to non-drifting concept presented by Dyakonov and Shur's group. In our previous reports, we just stated briefly and mentioned the derived results of effective permittivity and the calculated results.

In this paper, a generalized three dimensional (3D) TM mode analysis to analyze the characteristics of 2DEG drifting plasma at the AlGaAs/GaAs hetero-interface is presented in detail. It is noted here that the approach is also applicable to other III-V HEMT material systems. In Section 2, the determination of electromagnetic fields in semiconductor drifting plasma using the combination of well-known Maxwell's equations and carrier kinetic equation based on semiconductor fluid model is described. In this section, the derivation of the effective permittivity of drifting plasma in 2DEG on semi-insulating substrate is also presented. Next, the analysis to describe the presence of interactions using a so-called interdigital-gated high-electron-mobility-transistor (HEMT) plasma wave device is demonstrated in Section 3. Here, the admittance of the interdigital gate structure is calculated. In Section 4, a brief analysis and discussion on the Dyakonov-Shur THz surface wave in 2DEG is also presented. Finally, the conclusion is summarized in Section 5.

2. ELECTROMAGNETIC FIELDS IN 2DEG SEMICONDUCTOR DRIFTING PLASMA

In order to determine the electromagnetic fields in 2DEG semiconductor drifting plasma, the TM mode analysis of the plasma wave interactions for the device structure shown in Fig. 1 is performed basically following the procedures similar to those used in the semiconductor-insulator structure [10]. Here, we consider that a TM wave is propagating with a uniform electron flow in the z direction, with a drift velocity, v_d, along the 2DEG layer, embedded in semi-infinite GaAs and AlGaAs layers. A basic dispersion equation for TM waves can be derived by combining well-known Maxwell's equations with the equation of electron motion in the effective mass approximation based on

the fluid model of semiconductors indicated as follow;

$$\frac{d\vec{v}}{dt} = \frac{\partial \vec{v}}{\partial t} + \vec{v} \cdot \nabla \vec{v} = -\frac{q}{m^*}\left(\vec{E} + \vec{v} \times \vec{B}\right) - \frac{v_{th}^2}{n}\nabla n - \nu \vec{v}$$
$$\text{or} \quad \frac{d\vec{v}}{dt} = \frac{\partial \vec{v}}{\partial t} + \vec{v} \cdot \nabla \vec{v} = -\frac{q}{m^*}\left(\vec{E} + \mu_0 \vec{v} \times \vec{H}\right) - \frac{v_{th}^2}{n}\nabla n - \frac{\vec{v}}{\tau} \tag{1}$$

The Eq. (1) is obtained by applying the charge-current conservation principle derived from zeroth momentum term of Boltzman transport equation into the first momentum term of Boltzman transport equation. The left-hand side of Eq. (1) represents an acceleration term caused by external force applied to electrons. The first term, second term and third term of the right-hand side of Eq. (1) represents acceleration term caused by Lorentz force, diffusion term and the collision term, respectively. The acceleration term caused by Lorentz force was not considered in the Sumi's analysis [3]. The acceleration term caused by Lorentz force shows the inertia effect experienced by electrons when there is an introduction of external electromagnetic fields. The collision term shows the effect due to the collisions among the electrons or the collisions between the electrons and ionized impurities. The diffusion term show the diffusion effect due to the movement of electrons caused by electron temperature ambience.

To derive the electromagnetic fields in semiconductor drifting plasma, the following assumptions are applied. (a) Only one sort of carriers exists in the semiconductor layer, (b) the semiconductor layer is isotropic and (c) mobility is not changed with electric field. Basically, we generalized the TM mode analysis by Sumi [3] in such a way that the inertia effect of the electron in the nearly collision free

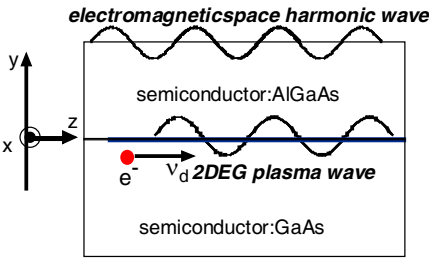

Figure 1. 2DEG AlGaAs/GaAs heterointerface and its coordinate.

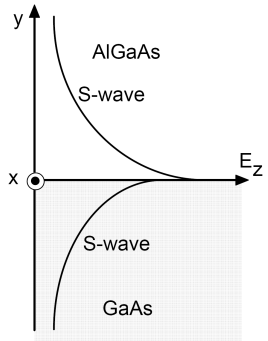

Figure 2. S-wave in AlGaAs/GaAs structure.

(NCF) situation is included. Since the collision frequency, ν, in the semiconductor plasma falls typically in the THz or sub-THz region at room temperature, and even in a lower frequency range at lower temperature, the NCF case is a realistic possibility.

Similarly to the case of semiconductor-insulator structure [10], it can be shown that only quasi-solenoidal surface wave (s-wave) components, which represent the solenoidal electromagnetic field distribution penetrating into the semiconductor region as well as that penetrating into the upper dielectric region, exist in the space, and the charge modulation in the 2DEG layer can be incorporated as a boundary condition connecting these two s-wave components, i.e., one in the lower semiconductor half-space and the other in the upper dielectric half-space. These two s-wave components are schematically shown in Fig. 2. It is also described for the case of semiconductor-insulator structure that if there is no diffusion of surface charge at the interface, then the component of electromagnetic wave is assumed to be only quasi-solenoidal component. In addition, the advantage of 2DEG structure is that the effect of lamellar component is very small due to the confinement of carriers in 2DEG layer.

As mentioned earlier, we assume that surface plasma waves propagate along the 2DEG layer with the phase factor of $\exp(j(\omega t - kz))$ in the z direction as shown in Fig. 1. Based on a standard field analysis, an expression for the ω- and k-dependent effective permittivity, $\varepsilon_{eff}(\omega, k)$, of the 2DEG plasma wave was derived as follow.

$$\varepsilon_{eff} = \varepsilon_{AlGaAs} \left(1 - \left(\frac{q^2 n_S}{m^* \varepsilon_{AlGaAs}}\right) \frac{k}{(\omega - k v_d)(\omega - k v_d - j\nu)} \frac{1}{1 - \frac{(k v_{th})^2}{(\omega - k v_d)(\omega - k v_d - j\nu)}}\right) \quad (2)$$

This effective permittivity will be applied for admittance calculation explained in Section 3, in order to describe the response of the semiconductor plasma to the TM surface wave excitation.

3. ADMITTANCE OF INTERDIGITAL-GATED SLOW WAVE STRUCTURE

3.1. Device Structure and Theoretical Formulation

The schematic physical device structure is shown in Fig. 3. In this section, the effective permittivity derived in Section 2, is utilized in the calculation of the two-terminal admittance of the interdigital structure shown in Fig. 3. For the calculation, we used a Green's function

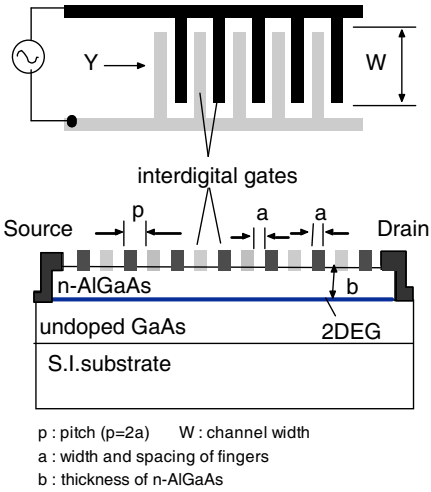

Figure 3. Physical device structure under study.

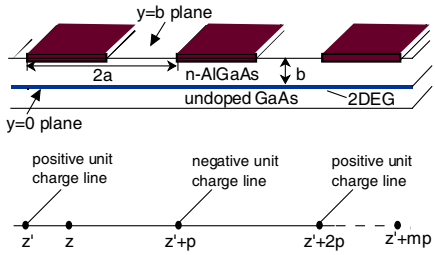

Figure 4. Schematic for admittance analysis of interdigital gates.

method [16]. Namely, with reference to Fig. 4, a periodic Green's function, $G_p(z, z')$, for the multiconductor strip lines was defined as the potential at point z on a metal finger in response to an array of the unit positive and negative charge lines placed at positions of $z'+mp$ with $m = 0, \pm1, \pm3, \pm5, \ldots$. Then, $G_p(z, z')$ was calculated as follows.

$$G_p(z,z') = \sum_{\substack{n=-\infty \\ \text{odd}}}^{\infty} \frac{\exp^{-jk_n(z-z')}}{|k_n|\, p(\varepsilon_o + \varepsilon^*_{eff}(\omega_n, k_n))}; \quad k_n = \frac{\pi}{p} n \ (n = \pm1, \pm3, \pm5, \ldots), \tag{3}$$

where ε_0 is the permitivity of vacuum and ε^*_{eff} is the effective permitivity of the 2DEG plasma. A Fredholm's integral equation of the first kind for the charge density function $\rho(z')$ at the point z' on the strip is obtained as follows.

$$\phi = \int_{finger} Gr(z,z')\rho(z')dz' \tag{4}$$

Then, the interdigital admittance was evaluated by solving that Fredholm's integral equation on a computer using matrix algebra [16] in order to obtain the charge distribution, $\rho(z')$ on the finger. Here, ϕ is the potential of the finger and $Gr(z, z')$ is a Green function for a strip line which is defined by the potential at point z in response to a point z' with a unit charge.

Finally, the interdigital two-terminal admittance was evaluated by the following equation,

$$Y = G + j\omega C = \frac{1}{\phi} \int_{finger} \rho(z) dz \tag{5}$$

where G and C are the conductance and capacitance of the interdigital structure loaded with 2DEG plasma, respectively.

3.2. Space Harmonics in Interdigital Slow-wave Structure

In this section, the basic characteristics of the interdigital slow-wave structure will be theoretically considered in terms of the existence of space harmonics in this structure. The cross-sectional structure for consideration is shown in Fig. 5. This structure is divided into three regions as follows:

Region I ($b \leq y < +\infty$): dielectric layer with dielectric permittivity constant, ε_0.

Region II ($0 \leq y < b$): dielectric layer with dielectric permittivity constant, ε_1.

Region III ($-\infty \leq y < 0$): semiconductor layer with dielectric permittivity constant, ε_2.

The channel of carrier flow is assumed to be at the plane of $y = 0$ and the interdigital slow-wave structure is assumed to be located at the plane of $y = b$ where its thickness is ignored (infinitely thin) and has a unit length in x direction. As shown in Fig. 5, these interdigital fingers are arranged in z direction. The difference of phase angle between two

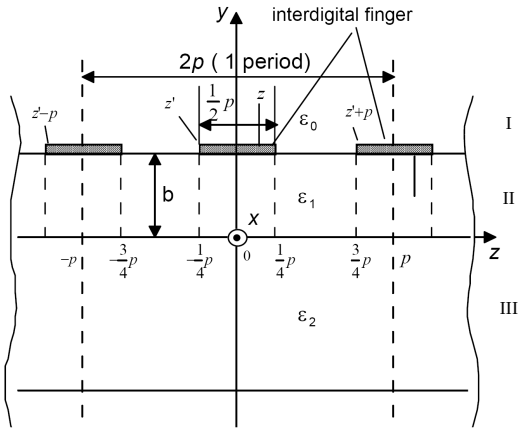

Figure 5. Schematic for space harmonic analysis of interdigital gates.

adjacent fingers is assumed to be equal to π. The electrons are also assumed to propagate as a space charge waves in a very thin layer of about 10 nm.

For simplicity, in this analysis of the space harmonics propagating through a slow-wave structure, it is assumed that there is no carrier flow in the channel. With respect to the existence of carrier flow, the mixing between the electromagnetic fields produced by carrier flow and the electromagnetic fields produced by slow-wave structure will result in the asymmetric of both field distribution and the center of field distribution will also be shifted according to the carrier drift velocity. Thus, this situation is hard to be considered in this analysis.

The field distribution is considered using the Poisson equation. Here, the dielectric layer is assumed to be isotropic and the field is also assumed to be distributed uniformly in the x direction. Hence, the operator, $\partial/\partial x$, can be ignored ($\partial/\partial x = 0$). The expression of field distribution using two-dimensional Poisson equation is written as follows.

$$\frac{\partial^2 \phi\,(y,z)}{\partial y^2} + \frac{\partial^2 \phi\,(y,z)}{\partial z^2} = -\frac{1}{\varepsilon}\rho\,(y,z) \tag{6}$$

Here, $\phi\,(x,z)$ is the potential, ε is the dielectric permittivity and $\rho\,(x,z)$ is the charge density.

The boundary conditions for the potential can be expressed as the following.

$$\text{(i)}\ \phi\,(y=+\infty,z)=0 \tag{7}$$

$$\text{(ii)}\ \phi\,(y=-\infty,z)=0 \tag{8}$$

$$\text{(iii)}\ \phi\,(y=+0,z)=\phi\,(y=-0,z) \tag{9}$$

$$\text{(iv)}\ \phi\,(y=b+0,z)=\phi\,(y=b-0,z) \tag{10}$$

Assuming that the charges only exist on the finger strips and no charges in the other parts when the electromagnetic waves is introduced into the interdigital slow-wave structure, the boundary conditions for electric flux, D are expressed as follows.

$$\text{(v)}\ D_{1y}\,(y=0,z)=D_{2y}\,(y=0,z)\,.\quad \varepsilon_1\frac{\partial\phi}{\partial y}\bigg|_{y=0}=\varepsilon_2\frac{\partial\phi}{\partial y}\bigg|_{y=0} \tag{11}$$

$$\text{(vi)}\ D_{0y}\,(y=b,z)-D_{1y}\,(y=b,z)=\rho\,(y=b,z)\,.$$

$$\varepsilon_0\frac{\partial\phi}{\partial y}\bigg|_{y=b}=\varepsilon_1\frac{\partial\phi}{\partial y}\bigg|_{y=b}=-\rho\,(y=b,z) \tag{12}$$

Then, the charge distribution is expressed as follows.

$$\rho\,(y,z)=P\,(z)\,\delta\,(y-b) \tag{13}$$

where $P(z)$ is the distribution charge density on the finger strip and $\delta(y-b)$ is the Dirac δ function.

By assuming that the charge distribution is represented by Eq. (13), then Eq. (6) is converted to the form as expressed in the following Eq. (14) by the Laplace equation.

$$\frac{\partial^2\phi}{\partial y^2}+\frac{\partial^2\phi}{\partial z^2}=0 \tag{14}$$

Generally, for periodic structure, the field distribution is expressed in terms of the superposition of space harmonic waves. Thus, the potential, ϕ^i and the charge density distribution, $P(z)$ can be written in the complex form as follows.

$$\phi^i(y,z) = \sum_{n=-\infty}^{\infty}\Phi_n^i(y)\,e^{-jk_nz} \tag{15}$$

$$P(z) = \sum_{n=-\infty}^{\infty}P_ne^{-jk_nz} \tag{16}$$

Here, i represents the Regions I, II and III, $\Phi_n^i(y)$ represents the potential amplitude of the nth order of space harmonics in the region i and P_n represents the charge density amplitude of the nth order of space harmonics. k_n is the propagation constant of the nth order of space harmonics. We assume that the phase angle difference of potential between two adjacent strip conductors or a half-pitch is equal to π, then the period of fundamental wave, T is expressed as $T=2p$. k_n is obtained as

$$k_n=n\frac{2\pi}{T}=\frac{n\pi}{p} \tag{17}$$

Then, Eqs. (15) and (16) can be converted to

$$\Phi_n^i(y) = \frac{1}{2p}\int_{-p}^{p}\phi^i(y,z)e^{jk_nz}dz \tag{18}$$

$$P_n = \frac{1}{2p}\int_{-p}^{p}P(z)e^{jk_nz}dz \tag{19}$$

Introduce $\Phi_n^i(y)$ into the Laplace equation of Eq. (14), then the following Eq. (20) is obtained.

$$\frac{\partial^2\Phi_n^i}{\partial y^2}-k_n^2\Phi_n^i=0 \quad (i=\mathrm{I},\mathrm{II},\mathrm{III}) \tag{20}$$

The amplitude of potential is expressed as follows.

$$\Phi_n^i(y)=A_n^ie^{j|k_n|y}+B_n^ie^{-j|k_n|y} \quad (i=\mathrm{I},\mathrm{II},\mathrm{III}) \tag{21}$$

Applying the boundary conditions of (i) $\sim$ (v) into Eqs. (15) and (21), then the potentials of each region are obtained as follows.

Region I,

$$\phi^I(y,z)=\sum_{n=-\infty}^{\infty}\frac{1}{2}\left(\left(1+\frac{\varepsilon_2}{\varepsilon_1}\right)e^{2|k_n|b}+\left(1-\frac{\varepsilon_2}{\varepsilon_1}\right)\right)A_n^{III}e^{-|k_n|y}e^{-jk_nz} \quad (22)$$

Region II,

$$\phi^{II}(y,z)=\sum_{n=-\infty}^{\infty}\frac{1}{2}\left(\left(1+\frac{\varepsilon_2}{\varepsilon_1}\right)e^{|k_n|y}+\left(1-\frac{\varepsilon_2}{\varepsilon_1}\right)e^{-|k_n|y}\right)A_n^{III}e^{-jk_nz} \quad (23)$$

Region III,

$$\phi^{III}(y,z)=\sum_{n=-\infty}^{\infty}A_n^{III}e^{|k_n|y}e^{-jk_nz} \quad (24)$$

Applying the boundary condition of (vi) into Eqs. (22) and (23), then A_n^{III} is obtained as follows.

$$A_n^{III}=\frac{2\varepsilon_1P_n}{|k_n|\left((\varepsilon_0+\varepsilon_1)(\varepsilon_1+\varepsilon_2)e^{|k_n|b}+(\varepsilon_0-\varepsilon_1)(\varepsilon_1-\varepsilon_2)e^{-|k_n|b}\right)} \quad (25)$$

The potential amplitude of space harmonics on the strip conductors at $y=b$ is expressed as follows.

$$\Phi_n^I(y=b)=\frac{1}{2}\left(\left(1+\frac{\varepsilon_2}{\varepsilon_1}\right)e^{2|k_n|b}+\left(1-\frac{\varepsilon_2}{\varepsilon_1}\right)\right)e^{-|k_n|b}A_n^{III}$$

$$=\frac{\varepsilon_2+\varepsilon_1\coth|k_n|b}{|k_n|(\varepsilon_2(\varepsilon_0+\varepsilon_1\coth|k_n|b)+\varepsilon_1(\varepsilon_1+\varepsilon_0\coth|k_n|b))}P_n=F(|k_n|)P_n \quad (26)$$

The potential amplitude of space harmonics on the strip conductor, $\Phi_n^I(y=b)$ and the harmonic amplitude of charge density distribution, P_n is related by

$$F(|k_n|)=\frac{\varepsilon_2+\varepsilon_1\coth|k_n|b}{|k_n|\left(\varepsilon_2\left(\varepsilon_0+\varepsilon_1\coth|k_n|b\right)+\varepsilon_1\left(\varepsilon_1+\varepsilon_0\coth|k_n|b\right)\right)_n} \quad (27)$$

Considering Eqs. (25) and (27), the potentials of each region are rewritten as follows.

Region I,

$$\phi^I(y,z)=\sum_{n=-\infty}^{\infty}F(|k_n|)P_ne^{|k_n|(y-b)}e^{-jk_nz} \quad (28)$$

Region II,

$$\phi^{II}(y,z)=\sum_{n=-\infty}^{\infty}F(|k_n|)P_n\frac{\varepsilon_1\cosh|k_n|y+\varepsilon_2\sinh|k_n|y}{\varepsilon_1\cosh|k_n|b+\varepsilon_2\sinh|k_n|b}e^{-jk_nz} \quad (29)$$

Region III,

$$\phi^{III}(y,z) = \sum_{n=-\infty}^{\infty} F(|k_n|) P_n \frac{\varepsilon_1 e^{|k_n|y}}{\varepsilon_1 \cosh|k_n| b + \varepsilon_2 \sinh|k_n| b} e^{-jk_n z} \quad (30)$$

If P_n value is known, then the field distribution of the periodic structure can be obtained. Assuming that the charge density distribution in the x direction is uniform, the potential at point z, $\phi(b,z)$ by referring to the unit charge at point z' as schematically shown in Fig. 4, is given by Green's function as follows.

$$\phi(b,z) = \int_{-\infty}^{\infty} Gr(z,z')\rho(b,z')\,dz' \quad (31)$$

According to the Floke's theorem, the charge density at $(b, z' + mp)$ point is obtained as follows. Assuming that the charge density at point (b, z') on the strip is $P(z')$, then the charge density at point $(b, z'+mp)$ $(m = 0, \pm1, \pm2, \pm3, \ldots)$ is given by $P(z' + mp)$.

$$\rho(b, z' + mp) = P(z' + mp) = e^{-jk_1 mL} P(z') = e^{-jm\pi} P(z') \quad (32)$$

Eq. (31) can be transformed to the following equation.

$$\begin{aligned} \phi(b,z) &= \int_{-\frac{p}{2}}^{\frac{p}{2}} \sum_{m=-\infty}^{\infty} Gr(z, z' + mp)\,\rho(b, z' + mp) dz' \\ &= \int_{-\frac{p}{2}}^{\frac{p}{2}} \left[\sum_{m=-\infty}^{\infty} Gr(z, z' + mp)\, e^{-jm\pi} \right] P(z')\, dz' \end{aligned} \quad (33)$$

Here, $-\frac{p}{2} \le z' \le \frac{p}{2}$.

On the other hand, the distribution $P(z)$ in the range of $-\frac{p}{2} \le z \le \frac{p}{2}$ is given by

$$P(z) = \begin{cases} 0 & (p/4 < |z| < p/2) \\ P(z) & (0 \le |z| \le p/4) \end{cases} \quad (34)$$

Considering an Eq. (34), the integral range of Eq. (33) becomes $-p/4 \le z' \le p/4$. Then, Eq. (33) is obtained as follows.

$$\phi(b,z) = \int_{-\frac{p}{4}}^{\frac{p}{4}} \left[\sum_{m=-\infty}^{\infty} Gr(z, z' + mp)\, e^{-jm\pi} \right] P(z')\, dz' \quad (35)$$

The above equation represents the potential at point (b, z) of a single strip conductor.

Here, the following definition is made.

$$G_p(z, z') = \sum_{m=-\infty}^{\infty} Gr(z, z' + mp)\, e^{-jm\pi} \quad (36)$$

As shown in Fig. 5, $G_p(z, z')$ represents the potential at point z with respect to the point $z' + mp$ for the array of positive unit charge line and negative unit charge line.

The charge distribution for the array of line charge is given by

$$P'(z) = \sum_{m=-\infty}^{\infty} \delta\left(z - \left(z' + mp\right)\right) e^{-jm\pi} \tag{37}$$

Here, $P'(z)$ is transformed as follows:

$$P'(z) = \sum_{n=-\infty}^{\infty} P'_n e^{-jk_n z} \tag{38}$$

Then, P'_n is obtained as below.

$$P'_n = \frac{1}{2p} \int_{-p}^{p} P'(z)\, e^{jk_n z} dz = \frac{1}{p} e^{jk_{2n+1} z'} \tag{39}$$

In this analysis, we found that only odd space harmonics propagates in the interdigital slow-wave structure.

From the Fourier transformation equation the charge distribution of the periodic structure is given by the following equation.

$$\rho' = \sum_{n=-\infty}^{\infty} \frac{1}{p} e^{jk_{2n+1}(z'-z)} \tag{40}$$

$G_p(z, z')$ is obtained by the following equation.

$$G_p\left(z, z'\right) = \sum_{n=-\infty}^{\infty} \frac{1}{p} F\left(|k_{2n+1}|\right) e^{jk_{2n+1}(z'-z)} \tag{41}$$

The integral equation that need to be solved in order to determine the potential of single strip conductor, V_0 is shown in the Eq. (42).

$$V_0 = \int_{-\frac{p}{4}}^{\frac{p}{4}} \left[\sum_{n=-\infty}^{\infty} \frac{1}{p} F\left(|k_{2n+1}|\right) e^{jk_{2n+1}(z'-z)} \right] P\left(z'\right) dz' \tag{42}$$

With respect to the above Fredholm integral equation, then we can determine the charge density distribution on the conductor strip, $P(z)$ and its n-th order of the space harmonic amplitude, P_n.

Finally, the potential distribution of periodic structure can be obtained.

3.3. Numerical Procedure to Solve Integral Equation

Solution of the integral Eq. (42) can be accomplished by applying matrix approximation method [16]. Let the conductor surfaces be thought to be subdivided into M longitudinal strips of finite width ΔZ_i in the range of $-p/4 \le z \le p/4$. Here, other parameters and their definitions are summarized as follows.

Z_i: middle point of subdivided strip width.

P_i: average charge density ($i = 1, 2, 3, \ldots, M$).

V_k: the average potential of all potential values on the strip at $z = z_k$ point where ($k = 1, 2, 3, \ldots, M$).

In accordance with the above statements, Eq. (42) is then can be expressed as follows.

$$\begin{aligned} V_k &= \sum_{i=1}^{M} \left(\sum_{n=-N}^{N} \frac{1}{p} F\left(|k_{2n+1}|\, e^{-jk_{2n+1}(Z_i - Z_k)} \right) \right) P_i \Delta Z_i \\ &= \sum_{i=1}^{M} \left(\sum_{n=-N}^{N} \frac{\Delta Z_i}{p} F\left(|k_{2n+1}|\, e^{-jk_{2n+1}(Z_i - Z_k)} \right) \right) P_i \end{aligned} \tag{43}$$

It is noted here that the harmonic components of Green's function in Eq. (42) are considered infinite while in Eq. (43), the harmonic components are considered in the large enough range of $n = -N$ to $n = N$.

Here, the following assumption is made.

$$G_{ki} = \sum_{n=-N}^{N} \frac{\Delta Z_i}{p} F\left(|k_{2n+1}| \right) e^{-jk_{2n+1}(Z_i - Z_k)} \tag{44}$$

Then, Eq. (43) may be written in the matrix equation form as follows.

$$[V_k] = [G_{ki}]\,[P_i] \tag{45}$$

$$\begin{bmatrix} V_1 \\ V_2 \\ . \\ . \\ . \\ . \\ V_M \end{bmatrix} = \begin{bmatrix} G_{11} G_{12} \cdots G_{1M} \\ G_{21} G_{22} \\ . \\ . \\ . \\ . \\ G_{M1} \cdots\cdots G_{MM} \end{bmatrix} \begin{bmatrix} P_1 \\ P_2 \\ . \\ . \\ . \\ . \\ P_M \end{bmatrix} \tag{46}$$

The average charge density, $[P_i]$ is obtained as follows.

$$[P_i] = [G_{ki}]^{-1}\,[V_k] \tag{47}$$

In accordance to $[G_{ki}]$, it is necessary to apply a determination of geometric-mean distance, R to find the distance between the

subdivided partitions of conductor strip. Here, two kinds of geometric-mean distance are determined:

(1) The geometric-mean distance between the two subdivided partitions where $z_i \neq z_k$ or in the condition of the so-called off-diagonal term.

(2) The geometric-mean distance in the subdivided partition itself where $z_i = z_k$ or in the condition of the so-called diagonal term.

In the condition of off-diagonal term, the geometric-mean distance between two subdivided partitions can be approximated to the distance between the middle points of those two subdivided partitions if the number of the subdivided partitions, M is large enough.

In the condition of diagonal term, the geometric-mean distance, R is obtained as follows.

$$R = \exp\left(\log \frac{p}{2M} - \frac{3}{2}\right) \tag{48}$$

As mentioned before, the strip conductor with a width of $p/2$ is divided into M partitions where these widths are named as $S_1, S_2, \ldots, S_i, \ldots, S_k, \ldots, S_M$. Z_i is a middle point of S_i and Z_k is a middle point of S_k. The geometric-mean distance, R is a distance between the point of Z_i and Z_k. Therefore, this R value reflects to parameter $(Z_i - Z_k)$.

In addition, G_{ki} can also be assumed as follows.

$$G_{ki} = G_{ik} \tag{49}$$

In this analysis of the space harmonics propagating through the interdigital-gate structure, it is assumed that there is no carrier flow in the channel. Then, we can just consider the electromagnetic fields is only produced by the interdigital-gate structure and the center of field distribution will not be shifted. Therefore the matrix $[G_{ki}]$ can be assumed symmetric. By considering that the potential on the conductor strip is constant where $V_k = V_0 =$ constant $(k = 1, 2, \ldots, M)$, then we determine the charge density, P_i of Eq. (47).

3.4. Appearance of Negative Conductance

Using the procedure mentioned in previous section, we have calculated the interdigital admittance of the present device numerically on a computer. Calculation was carried out for wide range of parameters and negative conductance was obtained in various cases.

It was found that large negative conductance values can be obtained under a condition when the drift velocity is close to the phase

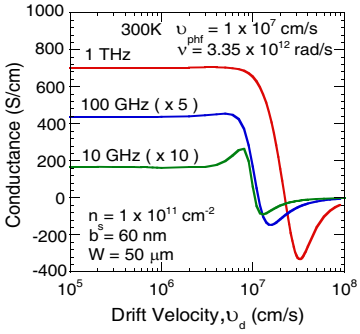

Figure 6. Calculated conductance as a function of drift velocity for 10 GHz, 100 GHz and 1 THz.

velocity, $\upsilon_{phf} = f(\text{frequency}) \times 2p$, of the fundamental space harmonic component of electromagnetic wave.

Examples of calculated conductance are plotted as a function of drift velocity for 10 GHz, 100 GHz and 1 THz at 300 K in Fig. 6 for the case of $\upsilon_{phf} = 1 \times 10^7$ cm/s, $n_{so} = 1 \times 10^{11}$ cm^{-2} and the AlGaAs thickness, $b = 60$ nm. Occurrence of negative conductance peak is seen when the electron drift velocity slightly exceeds phase velocity, υ_{phf}. Since the value of pitch, p, reduces with frequency for the same value of phase velocity, υ_{phf}, the available value of negative conductance per area is predicted to be very large, being of the order of 300 S/cm at 1 THz for $\upsilon_{phf} = 1 \times 10^7$ cm/s, $n_{so} = 1 \times 10^{11}$ cm^{-2} and $b = 60$ nm.

The value of negative conductance increases with increase of frequency and reduction of the AlGaAs thickness. The former is obviously related to the fact that the number of collision events per cycle is reduced as the frequency is increased. The calculation for other III-V HEMT material systems such as AlGaN/GaN material systems should also produce a similar tendency of results since the basic structure of both materials are same due to the basic equation of effective permittivity of both materials is same. The advantage of using AlGaN/GaN is that the breakdown voltage of this material is very high and may good for experiment since high drain-source voltage can be applied to drift the carriers along the channel. However, it is well known that this material produce large leakage for Schottky type contact which may affect the experimental results

As mentioned, we generalized the TM mode analysis by Sumi [3] in such a way that the inertia effect of the electron in the nearly collision free (NCF) situation is included. Since the collision frequency, ν, in the semiconductor plasma falls typically in the THz or sub-THz

region at room temperature, and even in a lower frequency range at lower temperatures, the NCF case is a realistic possibility. At high frequencies, a quantum mechanical treatment may become necessary. However, this is beyond the scope of our analysis. The existence of negative conductance for both of the collision-dominant (CD) case for microwave region and the nearly collision free (NCF) case for THz region are predicted which became remarkably large in the NCF case. Besides of III-V HEMT structure, small negative conductance are also obtainable in some other material systems such GaAs and InP bulk structure presented in reference [12]. However, the HEMT structure can be considered more preferable for plasma wave devices due to large negative conductance can be produced.

4. DYAKONOV-SHUR THz SURFACE WAVES IN 2DEG

Up to now, the terahertz band is still an unexplored region in the sense that no practical application exists. New operating principles by traveling wave concept should be, therefore, appreciated for the real applications. Recently, a new type of terahertz electronic device that utilizes the plasma resonance effect of highly dense two-dimensional electrons in the AlGaAs/GaAs heterostructure FET channel under a metal gate was proposed by Dyakonov and Shur [17].

The concept of devices proposed by Dyakonov and Shur utilizes the interaction of propagated plasma waves which may be much faster than electron drift velocities. Therefore, this principle should allow a three terminal device operation into a much higher frequency range than has been possible for conventional transit time limited regimes. The plasma resonance phenomena of such plasma wave device in the THz range were indirectly observed from the *dc*-modulation effect on the drain-source potential [18, 19].

In this section, we are going to describe the principles of such plasma resonance effect in FETs. Then, this theory is going to be compared and discussed with our approach concept.

4.1. Principles of Non-drifting Plasma Resonance Effect

The device structure used in their analysis is similar to the conventional high-electron-mobility transistors (HEMTs). The gate bias is applied to induce the highly dense 2DEG electrons of the order of $> 10^{12}\,\mathrm{cm}^{-2}$ in the channel, the average distance between electrons is close to the Bohr radius and a large number of electron-electron collisions occur during the electron transit time. When the HEMTs are biased only by the gate-to-source voltage and subjected to an electromagnetic

radiation which then will develop a constant drain-to-source voltage which has a resonant dependence on the radiation frequency with maxima at the plasma oscillation frequencies. Under such conditions, the electrons behave as a fluid and the electron motion can be described as plasma waves by hydrodynamic equations [8].

Due to the photon energy in the terahertz region is far smaller than the semiconductor band-gap energy, the terahertz electromagnetic wave can be absorbed via inter-and/or intra-subband transition of the two dimensional conduction electrons. When a terahertz electromagnetic wave having an E vector parallel to the channel axis (source-drain direction) is absorbed, a plasma wave of electrons is excited. If the subband-gap energy between the bound state and the second excited state is larger than the phonon energy, the plasma being excited via inter-subband transition can keep its coherency against the incoherence of phonon energy.

The plasma wave is carried on a uniform electron drift flow from the source to the drain electrode. This will cause the difference between the forward-wave velocity $(\upsilon_p + \upsilon_d)$ and the backward-wave velocity $(\upsilon_p - \upsilon_d)$ where υ_p is the plasma wave velocity and υ_d is the electron drift velocity. Corresponding to this situation, the plasma-wave instability will occur. The consequence of superimposing the multiple reflection waves leads to the wave amplitude of $\left(\left(\upsilon_p + \upsilon_d\right) / \left(\upsilon_p - \upsilon_d\right)\right)^{t/T}$ where T is the roundtrip time between the source and the drain. In general case, this will lead to a wave amplification when $\upsilon_p > \upsilon_d$. This is because υ_p is generally on the order of 10^8 cm/s for typical FET devices while υ_d stays at most on the order of 10^7 cm/s. That is the mechanism of plasma wave amplification. The standing wave condition is given by $\lambda = (2n-1)/4L$ (n: integer), where λ is the plasma wavelength and L is the gate length. For the high plasma wave velocity, υ_p (10^8 cm/s) and small FET dimensions, L (10^{-7} cm), the plasma wave frequencies, υ_p/λ are in the terahertz range.

4.2. Basic Properties of Dyakonov-Shur THz Surface Waves in 2DEG

The motion of plasma waves along with the z axis parallel to the source to drain direction can be described by the following hydrodynamic equations [8],

$$-q\frac{\partial V(z)}{\partial z} - m^*\frac{\upsilon}{\tau} = m^*\left(\frac{\partial \upsilon}{\partial t} + \upsilon\frac{\partial \upsilon}{\partial t}\right) \tag{50}$$

$$\frac{\partial V(z)}{\partial t} + \frac{\partial\left(V(z)\upsilon\right)}{\partial z} = 0 \tag{51}$$

where q is the electronic charge, $V(z)$ is the gate-channel potential at z, m^* is the electron effective mass, υ is the local electron velocity, τ is the plasma damping time. Eq. (50) is the Euler equation and Eq. (51) is the continuity equation in which the induced electronic charge is given by the product of the gate-channel potential, $V(z)$ and the uniform channel capacitance. The wave dispersion law, $\omega = S_0 k$ corresponding to the well known shallow water waves can be obtained from the linearized system of Eqs. (50) and (51) [17]. Then, the wave velocity, S_0 is obtained as follows.

$$S_0 = \sqrt{\frac{qV_G}{m^*}} \tag{52}$$

Here, ω is the frequency, k is the wave vector, and V_G is the gate bias potential.

In our approach, the dispersion relation of the TM surface waves can be obtained by matching the admittance at the interface (transverse resonance) [20]. By considering the "shallow water wave" — like plasma wave, then the dispersion can be obtained from the resonance relation as follows.

$$\frac{j\omega\varepsilon_{AlGaAs}}{\Gamma_s}\cot(kb)+\frac{j\omega}{\Gamma_s}\varepsilon_{AlGaAs}\left(1-\frac{\left(\omega_p^2 b\right)k}{\left(\omega-k\upsilon_d\right)\left(\omega-k\upsilon_d-j\nu\right)}\right)=0 \tag{53}$$

$$\frac{j\omega\varepsilon_{AlGaAs}}{k}\cot(kb)+\frac{j\omega}{k}\varepsilon_{AlGaAs}\left(1-\frac{\left(\omega_p^2 b\right)k}{\left(\omega-k\upsilon_d\right)\left(\omega-k\upsilon_d-j\nu\right)}\right)=0 \tag{54}$$

Here, b is the thickness of the AlGaAs layer. Assuming that $\omega \gg k\upsilon_d$, then Eq. (54) can be expressed as follows.

$$\frac{\varepsilon_{AlGaAs}}{kb}+\varepsilon_{AlGaAs}\left(1-\frac{\left(\omega_p^2 b\right)k}{\omega^2}\right)=0 \tag{55}$$

Assuming that $1 \ll \frac{\left(\omega_p^2 b\right)}{\omega^2}k$, then we obtain

$$\frac{\varepsilon_{AlGaAs}}{kb}=\frac{\varepsilon_{AlGaAs}\left(\omega_p^2 b\right)k}{\omega^2} \tag{56}$$

From the wave dispersion law, $\omega = S_0 k$ where S_0 is the wave velocity, we can obtain the following equation.

$$\omega^2=\frac{b\varepsilon_{AlGaAs}\left(\omega_p^2 b\right)}{\varepsilon_{AlGaAs}}k^2=S_0^2k^2 \tag{57}$$

Here, $S_0^2=\frac{b\varepsilon_{AlGaAs}\left(\omega_p^2 b\right)}{\varepsilon_{AlGaAs}}$.

By taking the limit $kb \to 0$ and ignoring diffusion ($\upsilon_{th} = 0$), a linear dispersion equation with the velocity, S_0 is obtained. Here, C is the gate capacitance per unit area, $\omega_p^2 b = \frac{q^2 n_S}{m^* \varepsilon_{AlGaAs}}$ and in the case of a gated 2DEG (i.e., of a FET), the relation between the electron concentration and electric potential is given by $qn_S = CV_G$.

$$S_0^2 = \frac{1}{C}\varepsilon_{AlGaAs}\frac{q^2 n_S}{m^* \varepsilon_{AlGaAs}} = \frac{1}{C}\frac{(qn_S)\, q}{m^*} = \frac{qV_G}{m^*} \tag{58}$$

It can be seen that Eq. (58) is equal to the Eq. (52) although our treatment is more rigorous that the one-dimensional analysis by Dyakonov and Shur [17, 18].

5. CONCLUSION

The generalized TM mode analysis method was applied to analyze the interactions in two-dimensional electron gas (2DEG) structure. The effective permittivity which is used to describe the dielectric response of the semiconductor plasma to the TM surface wave excitation was derived. The theoretical formulations and procedures to determine the admittance of the interdigital structure was presented. It was found that only the odd-mode space harmonics propagate through the interdigital slow-wave structure. The major result of our theoretical analysis is the appearance of negative conductance where its magnitude increases with the increase of frequency. This indicates that the best use of the wave interaction can be made by using the 2DEG structure in the THz region because of reduced collision, reduced thermal motion due to confinement, absence of surface states due to superb hetero-structure and increased number of fingers per unit length. The surface plasma wave mode in 2DEG in conventional HEMT structures, screened by a highly conducting plane, proposed by Dyakonov and Shur was briefly described and discussed. The plasma wave velocity proposed by Dyakonov and Shur can be obtained by equating the admittance at the interface.

ACKNOWLEDGMENT

This work was partly supported by Ministry of Science, Technology and Innovation (MOSTI), Malaysia and Ministry of Higher Education (MOHE), Malaysia through Science Fund 03-01-06-SF0283 and Fundamental Research Grant Scheme Vote 78205 & 78417, respectively.

REFERENCES

1. Solymar, L. and E. Ash, "Some travelling-wave interactions in semiconductors theory and design considerations," *Int. J. Electronics*, Vol. 20, No. 2, 127–148, 1966.
2. Hines, M. E., "Theory of space-harmonic traveling-wave interactions in semiconductors," *IEEE Trans. Electron. Devices*, Vol. 16, 88–97, 1969.
3. Sumi, M., "Traveling-wave amplification by drifting carriers in semiconductors," *Jpn. J. Appl. Phys.*, Vol. 6, 688–698, 1967.
4. The special issue on plasma wave interactions in semiconductors in the March 1970 issue of *IEEE Trans. Electron. Devices*, Vol. 17, 1970.
5. Yamashita, Y., A. Endoh, K. Shinohara, K. Hikasaka, T. Matsui, S. Hiyamizu, and T. Mimura, "Pseudomorphic $In_{0.52}Al_{0.48}As/In_{0.7}Ga_{0.3}As$ HEMTs with an ultrahigh f_T of 562 GHz," *IEEE Electron. Device Lett.*, Vol. 23, No. 10, 573–575, 2002.
6. Amano, Y., M. Kosugi, K. Kosemura, T. Mimura, and M. Abe, "Short-channel effects in subquarter-micrometer-gate HEMTs: Simulation and experiment," *IEEE Trans. Elctron. Devices*, Vol. 36, No. 10, 2260–2266, 1989.
7. Sano, E., "Simulation of nanoscale InAlAs/InGaAs high electron mobility transistors based on drift-diffusion model incorporating an effective potential," *Jpn. J. Appl. Phys.*, Vol. 42, No. 7A, 4261–4263, 2003.
8. Dyakonov, M. and M. Shur, "Shallow water analogy for a ballistic field effect transistor. New mechanism of plasma wave generation by DC current," *Phys. Rev. Lett.*, Vol. 71, 2465–2468, 1993.
9. Otsuji, T., Y. Kanamaru, H. Kitamura, M. Matsuoka, and O. Ogawara, "Effect of heterostructure 2-D electron confinement on the tunability of resonant frequencies of terahertz plasma-wave transistors," *IEICE Trans. Electron.*, Vol. E86-C, 1985–1993, 2003.
10. Hashim, A. M., "Plasma waves in semiconductors and their interactions with electromagnetic waves up to THz region," Ph.D. Thesis, Hokkaido University, Japan, 2006.
11. Hashim, A. M., S. Kasai, and H. Hasegawa, "Observation of third harmonics response in two-dimensional AlGaAs/GaAs HEMT devices due to plasma wave interaction," *Superlattices and Microstruct*, Vol. 44, 754–760, 2008.
12. Iizuka, K., A. M. Hashim, and H. Hasegawa, "Surface plasma wave

interactions between semiconductor and electromagnetic space harmonics from microwave to THz range," *Thin Solid Films*, Vol. 464–465, 464–468, 2003.

13. Hashim, A. M., T. Hashizume, K. Iizuka, and H. Hasegawa, "Plasma wave interactions in the microwave to THz range between carriers in a semiconductor 2DEG and interdigital slow waves," *Superlattices Microstruct*, Vol. 34, 531–537, 2003.
14. Hashim, A. M., S. Kasai, T. Hashizume, and H. Hasegawa, "Integration of interdigital-gated plasma wave device for proximity communication system application," *Microelectronics Journal*, Vol. 38, 1263–1267, 2007.
15. Hashim, A. M., S. Kasai, K. Iizuka, T. Hashizume, and H. Hasegawa, "Novel structure of GaAs-based interdigital-gated HEMT plasma devices for solid-state THz wave amplifier," *Microelectronics Journal*, Vol. 38, 1268–1272, 2007.
16. Seki, S. and H. Hasegawa, "Analysis of crosstalk in very high-speed LSI/VLSI's using a coupled multiconductor MIS microstrip line mode," *IEEE Trans. MTT*, Vol. 32, 1715–1720, 1984.
17. Dyakonov, M. and M. S. Shur, "Detection, mixing, and frequency multiplication of terahertzradiation by two-dimensional electronic fluid," *IEEE Trans. Electron. Devices*, Vol. 43, 380–387, 1996.
18. Knap, W., Y. Deng, S. Rumyantsev, J. Q. Lu, M. S. Shur, C. A. Saylor, and L. C. Brunel, "Resonant detection of subTHz radiation by plasma waves in a submicron field-effect transistor," *Appl. Phys. Lett.*, Vol. 80, 3433–3435, 2002.
19. Hashim, A. M., S. Kasai, and H. Hasegawa, "Observation of third harmonics response in two-dimensional AlGaAs/GaAs HEMT devices due to plasma wave interaction," *Superlattices and Microstructures*, Vol. 44, 754–760, 2008.
20. Hasegawa, H., M. Furukawa, and H. Yanai, "Properties of microstrip line on Si-SiO_2 system," *IEEE Trans. Microwave and Theory Technique*, Vol. 19, 869–881, 1971.